

Searches for Resonances at the LHC

Edward Moyses

Department of Physics, University of Massachusetts, 710 North Pleasant St, Amherst, USA

On behalf of the ATLAS and CMS Collaborations

Data taken in 2011 with the ATLAS and CMS detectors at the LHC have been used to search for resonances. Results are presented based on up to 5 fb^{-1} of $\sqrt{s} = 7 \text{ TeV}$ proton-proton collisions in final states which include dileptons, diphotons, dijets, jets+photons, dibosons, MET+charged lepton and $t\bar{t}$. No evidence of new physics is seen, but limits have been placed on various benchmark models.

1 Introduction

Many proposed extensions to the Standard Model (SM) of particle physics are expected to be expressed in heavy resonances visible at the LHC. These proceedings detail the search for resonances with the ATLAS¹ and CMS² detectors, using data taken from the 2011 LHC run.

No excesses were seen, so the following will concentrate on documenting the latest limits, grouped together via various final state topologies (and which are listed in approximate order of experimental complexity): dileptons; diphotons; dijets; jets+photons; diboson; MET+charged leptons; ditop ($t\bar{t}$).

The results are interpreted in terms of benchmark models, but most limits are presented in a general way and can therefore be interpreted in other models. The benchmarks used include: the Randall-Sundrum (RS) model, which predicts a tower of Kaluza-Klein (KK) excitations of the graviton/gluon; a Z' , either from the Sequential Standard Model (SSM), where the new gauge bosons are assumed to have SM-like couplings, or from additional large symmetry groups (such as E6); or finally, a generic resonance with a mass and width.

2 Dilepton resonances

Dilepton final states are characterised by very clean signatures and are predicted by SM-extensions including: extra heavy gauge bosons, techni-mesons, and RS gravitons. Figure 1 shows the $\mu\mu$ mass spectra for ATLAS using 5 fb^{-1} of data, as well as the stacked sum of background processes (of which Drell-Yan is the most significant component)³. Mass spectra are consistent with expectations from SM, and so in Table 1 the newest limits are shown, whilst Figure 2 shows the CMS 95% Confidence Limits (CL) for various benchmark models in 4.9 fb^{-1} ⁴.

3 Diphoton resonances

In addition to their clean signature, the branching ratio (BR) for spin-2 gravitons decaying to diphotons is double that to lepton final states. The main irreducible background is SM

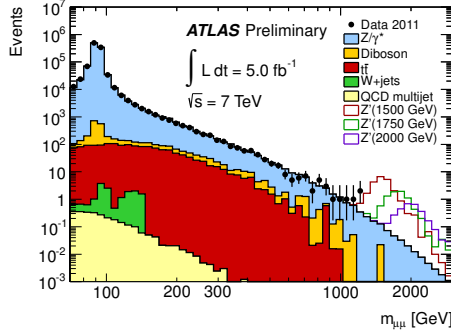


Figure 1: Invariant mass spectrum of dimuon events for ATLAS. The points with error bars represent the data. The uncertainties on the data points (stat. only) represent 68% confidence intervals for the Poisson means. The histograms represent the SM expectation³.

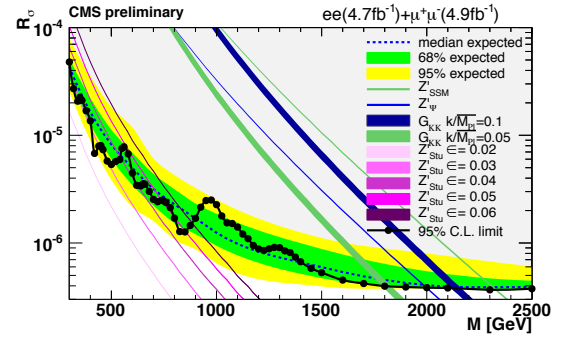


Figure 2: Upper limits on the production ratio $\sigma \times BR$ of cross section times branching fraction into $\mu\mu/ee$ pairs for Z'_{SSM} , Z'_{Ψ} , and G_{KK} production. Shaded yellow (red) bands correspond to the 68% (95%) quantiles for the expected limits⁴.

$\gamma\gamma$ production (estimated by simulation), whilst the reducible component consists mainly of γ +jet and jet+jet (estimated from data). With 2.2 fb^{-1} CMS excludes a RS graviton with mass less than $0.86(1.84) \text{ TeV}$ for couplings $k/\bar{M}_{PL} = 0.01(0.1)$ ⁵, whilst with 2.12 fb^{-1} (and in combination with the dilepton result) ATLAS excludes masses less than $0.80(1.95) \text{ TeV}$ for $k/\bar{M}_{PL} = 0.01(0.1)$ ⁶.

4 Dijet resonances

Dijets are sensitive to a variety of beyond-SM physics, such as string resonances, excited quarks, RS gravitons etc. The exclusions for excited quarks in ATLAS⁷ are shown in Table 1 (CMS has also excluded: $m_{q^*} < 2.49 \text{ TeV}$; String Resonances $< 4.00 \text{ TeV}$; E6 Diquarks $< 3.52 \text{ TeV}$; and Axiglons/Colorons $< 2.47 \text{ TeV}$ ⁸). ATLAS's invariant mass distribution and CL are shown in Figures 3 and 4 respectively. ATLAS used 4.8 fb^{-1} of data, whilst CMS used 1.0 fb^{-1} .

5 Photon plus Jet resonances

The benchmark model is an excited quark, and with this final state and 2.11 fb^{-1} of data, ATLAS has excluded⁹ a q^* with mass less than 2.46 TeV .

6 Diboson resonances

For the beyond-SM graviton mediated ZZ resonances, there are two final states consider: $llll$ and $lljj$. The ATLAS graviton mass limits¹⁰, produced with 1.02 fb^{-1} , are shown in Table 1, whilst the CL plot is shown in Figure 5. It is also possible to look for resonant structure in decay of $WZ \rightarrow ll\nu$, predicted, for example, by Low Scale Technicolor Model. The CMS ρ_{TC} mass limits¹¹, produced with 4.7 fb^{-1} , are shown in Table 1, whilst the CL plot is shown in Figure 6. ATLAS has also excluded¹² a ρ_{TC} with mass less than 467 GeV (using 1.02 fb^{-1}).

7 $t\bar{t}$ resonances

Topcolor Z' decays preferentially to t or u , whilst the chosen RS KK gluon models couple more strongly to the top than other SM particles. Various final states have been considered: all-hadronic (6 jets); semi-leptonic (qqb)($\mu\nu b$); dilepton. As the decay products are boosted, jets can merge so the analyses must look for 'subjets' and use different algorithms depending on

Table 1: Some of the newer limits set at the LHC. See the referenced texts for more details.

Final state	Experiment	Mass Limits (GeV)	
Dilepton	ATLAS	$Z'_{SSM} > 2210$	$RS G_{KK} > 2160$ for $k/\bar{M}_{PL} = 0.1$
	CMS	$Z'_{SSM} > 2320$	$RS G_{KK} > 1810(2140)$ for $k/\bar{M}_{PL} = 0.05(0.1)$
Dijet	ATLAS	$q^* > 3350$	
Diboson	ATLAS ZZ	$RS G_{KK} > 845$ or < 325 for $k/\bar{M}_{PL} = 0.1$	
	CMS WZ	$W'_{SSM} > 1141$	$\rho_{TC} > 935$ or < 180
$t\bar{t}$	ATLAS l+jets	$Z'_{SSM} > 860$ or < 500	$g_{KK} > 1025$ or < 500
	CMS all-had.	$Z'_{TC} < 1000$ or > 1600 (width $\Gamma_{Z'}/m_{Z'} = 3\%$)	

the event topology. Figure 7 shows the CMS limits for Z' for the all-hadronic channel¹³ in 4.6 fb^{-1} , whilst new ATLAS limits using lepton+jets¹⁴ and 2.05 fb^{-1} are shown in Table 1 and Figure 8. Using 4.33 fb^{-1} of data in the e+jets channel, CMS has put a limit of 2.51 pb for Z' mass of 1 TeV ¹⁵. Finally, with 1.04 fb^{-1} ATLAS¹⁶ has used the dilepton channel to exclude $m_{g_{KK}} < 840 \text{ GeV}$.

References

1. ATLAS Collaboration, *The Atlas Experiment at the CERN Large Hadron Collider*, JINST **3** (2008) S08003.
2. CMS Collaboration, *The CMS Experiment at the CERN Large Hadron Collider*, JINST **3** (2008) S08004.
3. ATLAS Collaboration, ATLAS-CONF-2012-007, <https://cdsweb.cern.ch/record/1428547>.
4. CMS Collaboration, PAS_EXO-11-019, <https://twiki.cern.ch/twiki/bin/view/CMSPublic/PhysicsResultsEXO11019Winter2012>.
5. CMS Collaboration, arXiv:1112.0688
6. ATLAS Collaboration, *Phys. Lett. B* **710**, 538-556 (2012)
7. ATLAS Collaboration, ATLAS-CONF-2012-038, <https://cdsweb.cern.ch/record/1432206>
8. CMS Collaboration, *Phys. Lett. B* **704**, 123 (2011)
9. ATLAS Collaboration, arXiv:1112.3580 (submitted to *Phys. Rev. Lett.*)
10. ATLAS Collaboration, arXiv:1203.0718 (submitted to *Phys. Lett. B*)
11. CMS Collaboration, CMS-PAS-EXO-11-041, <https://twiki.cern.ch/twiki/bin/view/CMSPublic/PhysicsResultsEXO11041Winter2012>
12. ATLAS Collaboration, arXiv:1204.1648 (submitted to *Phys. Rev. D*)
13. CMS Collaboration, arXiv:1204.2488
14. ATLAS Collaboration, ATLAS-CONF-2012-029, <https://cdsweb.cern.ch/record/1430738>
15. CMS Collaboration, CMS-PAS-EXO-11-092, <https://cdsweb.cern.ch/record/1423037>
16. ATLAS Collaboration, ATLAS-CONF-2011-123, <https://cdsweb.cern.ch/record/1376423>

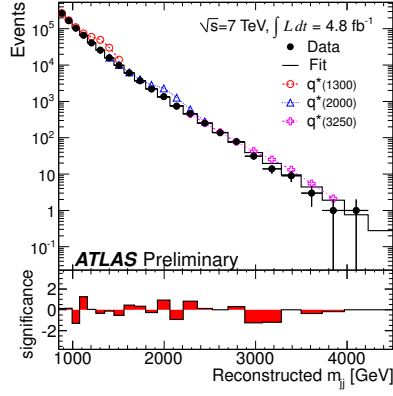


Figure 3: The reconstructed dijet mass distribution (filled points) fitted with a smooth functional form (solid line). Mass distribution predictions for three excited quark masses are shown above the background. The bin-by-bin significance of the data-background difference is shown in the lower panel ⁷.

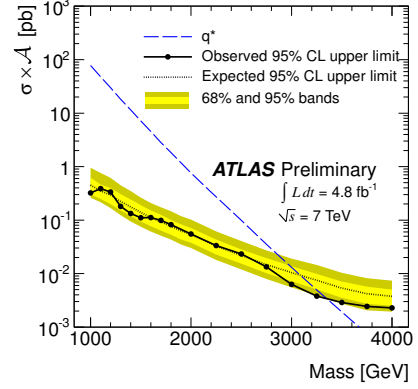


Figure 4: The 95% CL upper limits on $\sigma \times A$ as a function of particle mass (black filled circles) for excited quarks. The black dotted curve shows the 95% CL upper limit expected from Monte Carlo and the light(dark) yellow shaded bands represent the 68% (95%) contours of the expected limit ⁷.

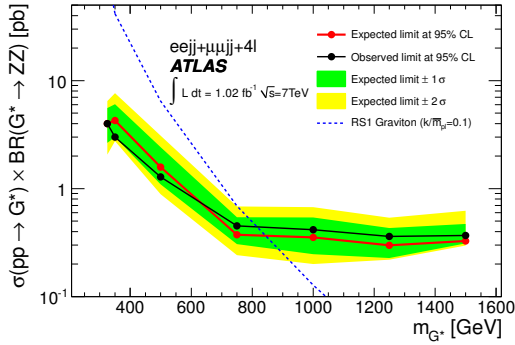


Figure 5: Expected and observed 95% CL limits for G^* to ZZ for the combined $lljj+llll$ channels. The leading-order theoretical prediction is also shown for $k/m_p l = 0.1$ ¹⁰.

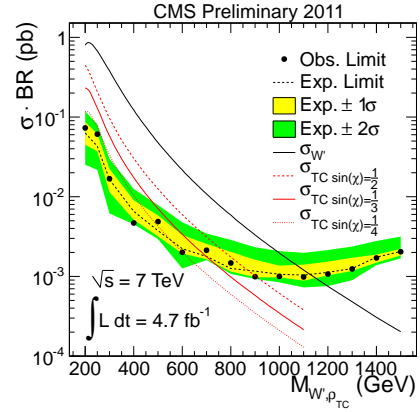


Figure 6: Expected and observed upper limit on $\sigma \times BR$ for W' and ρ_{TC} ¹¹.

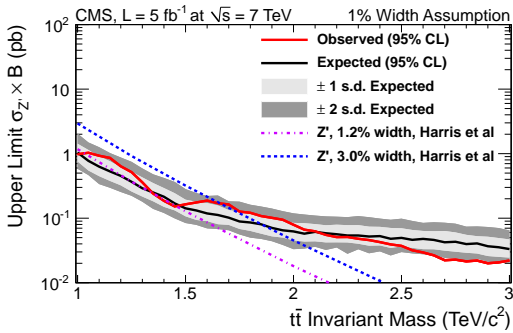


Figure 7: Limits on the possible cross section times branching ratio of $t\bar{t}$ resonances. This plot uses Z' sample with 1% width assumption ¹³.

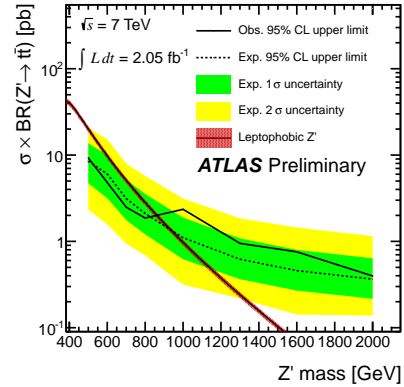


Figure 8: Limits on the possible $\sigma \times BR$ of $t\bar{t}$ resonances. This plot uses Z' sample with 1% width assumption. Expected (dashed line) and observed (solid line) upper limits on $\sigma \times BR$ ($Z \rightarrow t\bar{t}$). The red lines correspond to the predicted $\sigma \times BR$ for the leptophobic model ¹⁴.